

# Experimental comparison of non-contact and tactile R-test instruments in dynamic measurement

**Soichi Ibaraki. Koki Onodera**

Graduate School of Advanced Science and Engineering,  
Hiroshima University,  
Kagamiyama 1-4-1, Higashi Hiroshima, Hiroshima 739-8527, Japan  
E-mail: [ibaraki@hiroshima-u.ac.jp](mailto:ibaraki@hiroshima-u.ac.jp) (S. Ibaraki)

**Wen-Yuh Jywe, Chia-Ming Hsu, Yu-Wei Chang**

Department of Mechanical Engineering, National Taiwan University, ROC Taiwan.

**Abstract.** The R-Test measures the three-dimensional displacement of a tool center point with respect to a work table in five-axis machine tool, as linear axes are driven synchronously with a rotary axis. This paper experimentally compares the measuring performance of the R-Test instruments with 1) tactile linear displacement sensors, 2) laser displacement sensors based on the refraction in a glass ball lens (Laser R-Test), and 3) laser interferometers, in dynamic tests described in ISO 10791-6:2014. A tactile displacement sensor pushes its measuring contact to the target surface by a spring, and its stiffness can limit the measurement bandwidth. This paper experimentally investigates this influence in the measurement of dynamic synchronization error of rotary and linear axes particularly near the reversal point in the present tests. This paper also presents a test to measure the bandwidth of a tactile displacement sensor.

**Keywords:**

R-Test; five-axis machine tools; dynamic measurement; geometric errors.

## 1. Introduction

The radial, axial and tilt error motions of a rotary axis are typically measured by placing a spherical or cylindrical artefact on the axis of rotation, as is described in ISO 230-7 [1]. In a five-axis machine tool, such a setup may not be possible or difficult. For example, a swivel axis to tilt a rotary table may have its axis of rotation below the table surface. In such a configuration, a special fixture is needed to place a sphere on the axis of rotation. For such cases, the R-Test is accepted in ISO 10791-1 [2]. The application of the R-test to the error calibration of a five-axis machine tool was first reported by Weikert [3] and Bringmann and Knapp [4]. In typical R-Test setups, a precision sphere is attached to a machine spindle, and the sensors nest is installed on work table (an opposite setup is possible). As the rotary axis rotates, linear axes are synchronously driven on a circular path such that there exists nominally no displacement of the sphere with respect to the sensors nest. The sensors nest continuously measures the sphere's three-dimensional (3D) displacement. Bringmann et al. [4] and Ibaraki et al. [5] presented the identification of position and orientation errors of rotary axis average lines based on the static R-Test. Ibaraki et al. [5, 6] further extended it to position-dependent error motions of two rotary axes and presented a software to perform this assessment [7]. Commercial products are currently being offered by the likes of IBS Precision Engineering [8]. Many of dynamic interpolation tests for rotary axes described in ISO 10791-6 [9] can be done using the R-Test.

While many pioneering works [3, 4, 5, 10, 11] employed tactile linear displacement sensors for the R-Test, some works presented non-contact R-Test instruments. The commercial R-Test instrument by IBS Precision Engineering [8] is non-contact. Zargarbashi and Mayer [12] presented an R-Test instrument with non-contact capacitive sensors. Hong and Ibaraki [13] and Guo et al [14] presented a non-contact R-Test instrument by using a triangulation-based laser displacement sensor. Jiang et al. [15] employed eddy current displacement sensors.

Past works [13, 15] discussed potential advantages with non-contact linear displacement sensors: a contact linear displacement sensor is subject to the friction between the contact surface and a sphere, which can potentially cause the measurement uncertainty. Furthermore, more importantly, a contact linear displacement sensor typically has a spring to push its plunger to the target. The spring's stiffness can limit the measurement bandwidth.

On the other hand, drawbacks with non-contact linear displacement sensors include shorter working distance and measurable range. Capacitive and eddy current displacement sensors typically have the working distance  $\leq 1\text{mm}$  and the measurable range  $\leq 3\text{ mm}$ [12], which increases a risk of unwanted interference in machine operation or setup. An optical displacement sensor, e.g. a triangulation-based laser displacement sensor, can have longer working distance, but it is well recognized that a triangulation-based laser displacement sensor is typically subject to noise-like higher frequency measurement error, due to the laser beam speckle [16, 13].

Considering potentially limited bandwidth of tactile displacement sensors, non-contact displacement sensors have a potential advantage particularly in a dynamic test. No past works, however, have presented their experimental comparison. The objective of this paper is to experimentally compare the measuring performance of tactile and non-contact R-test instruments in a dynamic test.

In the literature, the R-Test has been often applied to the static measurement of rotary axis geometric errors. Fewer works have studied its application to dynamic tests. Nishiguchi et al. [17, 18] dynamically measured the synchronous error of a rotary axis and two linear axes, when the rotary axis reverses its rotation direction. They showed that this error is caused by the difference in the transient response of rotary and linear axes, and can cause a “scratch” on the finished surface of a significant depth (about 30  $\mu\text{m}$  in [17]). To measure this error, they employed a non-contact R-Test instrument using a triangulation-based laser displacement sensor. Jiang et al. [19] applied a contact-type R-Test to dynamically measure the 3D contour error for a “8-shaped” path within its measurable range. They did not study the measurement uncertainty of the contact-type displacement sensor in the dynamic test. The influence of the dynamic synchronous error of a rotary axis to linear axes can be often observed in five-axis machining tests. In the S-shape machining test, described in ISO 10791-7 [20], a “scratch” can be often observed on the finished surface due to the dynamic synchronization error induced by the five-axis singularity [21, 22]. Li et al. [23] presented a machining test designed to observe the influence of the dynamic synchronization error under the reversal of rotation direction. These works clearly show potentially significant influence of the dynamic synchronous error of rotary and linear axes on the machining accuracy.

Several different non-contact displacement measuring principles are available. This paper compares the following two sensors: 1) a laser displacement sensor based on the refraction in a glass sphere (Laser R-Test) and 2) a laser interferometer. 1) Laser R-Test, commercially available from Prof. Jywe Wen-Yuh’s Group, Department of Mechanical Engineering, National Taiwan University [24, 25, 26], measures the 3D displacement of a glass sphere, installed on the work table, by measuring the refraction of two orthogonally aligned laser beams going through the glass sphere. 2) A laser interferometer is often subject to smaller measurement noise than other laser displacement sensors, but its cost is significantly higher than 1). The major test objective is to compare the measuring performance of a tactile R-Test instrument with 1) and 2), to observe if the friction and the spring stiffness give significant influence on dynamic R-Tests in practical test conditions. The bandwidth of the tactile R-Test instrument is also experimentally measured.

## 2. Measuring instruments

### 2.1. Tactile R-Test instrument

Figure 1 show the tactile R-Test instrument tested in this paper. Three contact linear displacement sensors, ST1288 by Heidenhain, are installed in the sensors nest. The major specifications of the linear displacement sensor are shown in Table 1. Figure 2 shows its configuration [27]. The plunger is pushed to the target by the leaf spring. The sensor has a flat-ended measuring contact (carbide, contact surface size:  $\phi 4.8$  mm). A ceramic precision sphere with nominal diameter of 25.4 mm was attached to the spindle (diameter tolerance:  $\pm 1 \mu\text{m}$ , sphericity tolerance:  $0.13 \mu\text{m}$  (ABMA Grade GR5)). Compared to the machine's positioning uncertainty, this sphericity error of the sphere is sufficiently small.

The following parameters must be calibrated in advance: 1) unit vectors representing the sensor directions, and 2) the position of the sphere center from the spindle axis average line. See [5, 7] for further details of these pre-calibrations.

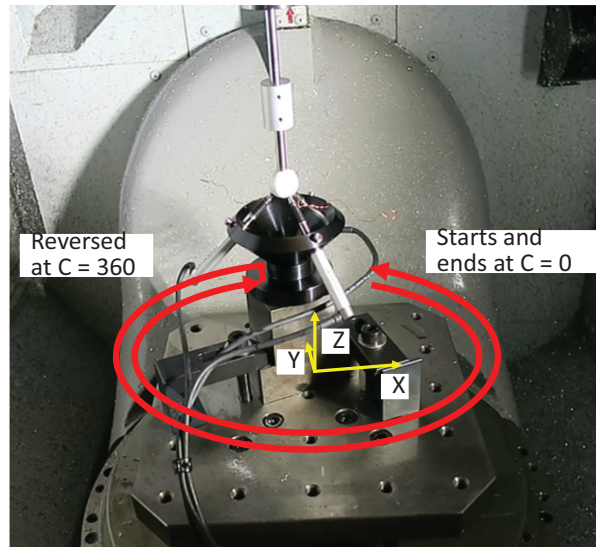
### 2.2. Laser R-Test

Figure 3 show the Laser R-Test. Figure 4 illustrates its measuring principle. The Laser R-Test head, installed on a machine spindle, has two laser beam sources (LS) aligned orthogonal to each other. The displacement of the glass ball lens (BL) in the direction normal to the laser beam can be estimated by measuring the displacement of the incident light by the quad-detector (QD) (Fig. 4 b). Table 2 shows its major specifications. Longer working distance, thus safer operation, relatively smaller measurement noise than other optical displacement sensors, and simpler configuration, and thus lower manufacturing cost, are its major advantages. The glass BL of the nominal diameter 8 mm was used as the target.

### 2.3. R-Test with laser interferometers

A laser interferometer, Keyence SI-F10, was employed. Table 3 shows its major specifications. Figure 5 shows the test setups. Since only one sensor is available, the sensor is installed on the work table in the a) tangential, b) radial, and c) axial direction of the rotary axis to be tested. A tungsten-carbide sphere with anti-reflection coating (the diameter:  $20.000 \text{ mm} \pm 2.5 \mu\text{m}$ , the calibrated sphericity:  $0.17 \mu\text{m}$ ) was installed on the machine spindle. Such separate measurement setups for radial, tangential and axial directions are described in ISO 10791-6 [9], which can be seen equivalent to the R-Test with three displacement sensors within the machine tool's repeatability.

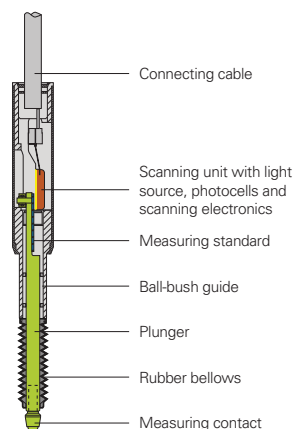
Hong et al. [13] compared the measuring performance of four different laser displacement sensors, 1) spectral interferometer (SI-F10, Keyence), 2) triangulation-based using specular reflection (LK-G10, Keyence), 3) triangulation-based using diffuse reflection (LK-H052, Keyence), and 4) confocal (LT-9010MS, Keyence) in scanning measurement of a spherical surface. Their tests showed that the interferometer, SI-F10,



**Figure 1.** C-axis test setup with the tactile R-Test instrument.

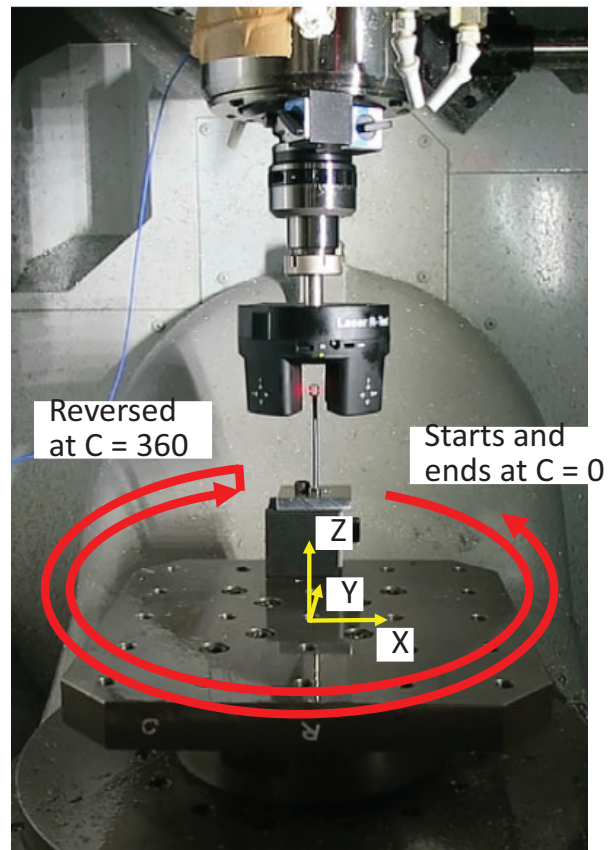
**Table 1.** Major specifications of linear displacement sensor used in the tactile R-Test instrument (ST1288 by Heidenhain [27]).

Measuring principle	Photo-electric scanning of an incremental scale with spring-tensioned plunger
Measurement range	12 mm
Signal pitch	20 $\mu\text{m}$
System accuracy	$\pm 1 \mu\text{m}$



**Figure 2.** Configuration of the tactile linear displacement sensor, ST1288 by Heidenhain [27].

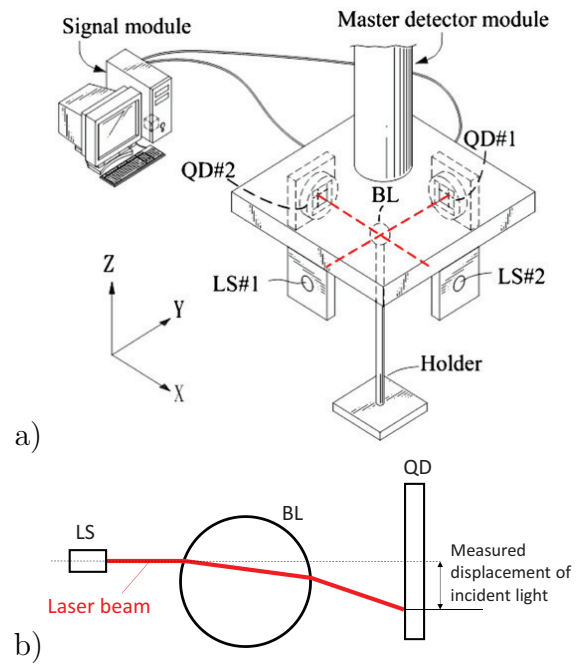
has significantly smaller noise-like higher frequency measurement error. Its drawbacks include higher sensitivity to the inclination of the target surface, and higher cost.



**Figure 3.** C-axis test setup with Laser R-Test.

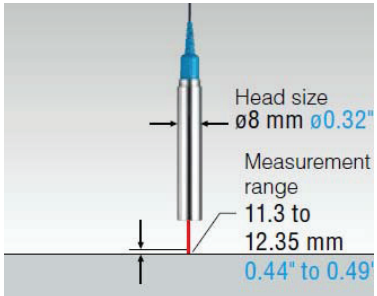
**Table 2.** Major specifications of Laser R-Test.

Resolution	$0.05 \mu\text{m}$
Measurable range	$\pm 0.1 \text{ mm}$
System accuracy	$0.5 \mu\text{m}$



**Figure 4.** Measuring principle of Laser R-Test [24]. LS: laser source, QD: quad-detector, BL: ball lens. a) Configuration. b) Principle of measuring the displacement of the BL.

**Table 3.** Major specifications of the interferometry-based laser displacement sensor, Keyence SI-F10 [28].

Measuring principle	Spectral interferometry
Measurement range	1.05 mm
Resolution	10 nm
Linearity	0.3 $\mu\text{m}$
Dimensions	

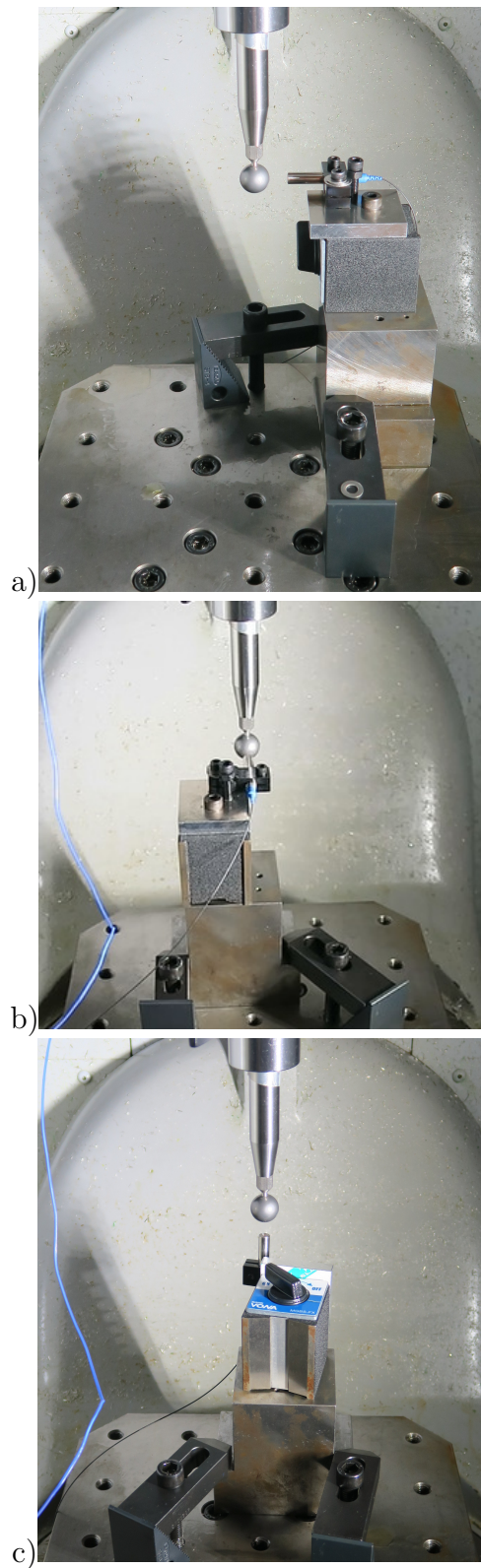


**Figure 5.** C-axis test setups with the laser interferometer. a) In tangential direction of C-axis, b) in radial direction, c) in axial direction.



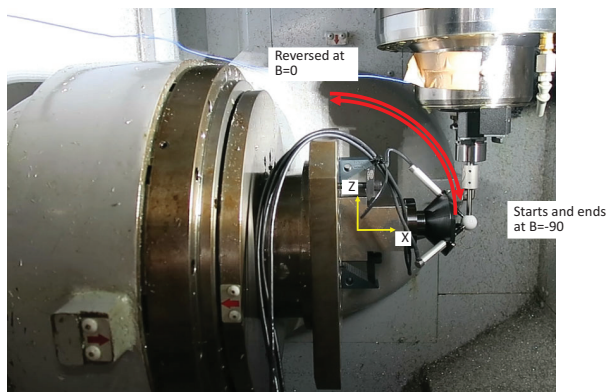


**Figure 6.** B-axis test setup with the contact R-Test instrument.

### 3. Test procedure

The machine tool has a rotary table (C-axis), mounted on a swivel axis (B-axis), in the workpiece side. The test procedure is in accordance with ISO 10791-6:2014 [9], Annex B ((1) in BK2 and (2) in BK1).

#### (1) Dynamic measurement of C-, X- and Y-axes synchronized motion

Figures 1 (with the tactile R-Test), 3 (for the Laser R-Test), and 5 (with the laser interferometer) show the test setups. C-axis is rotated from  $C = 0^\circ$  to  $360^\circ$ , and then to  $0^\circ$ . X- and Y-axes are synchronously driven with C-axis such that the tool center point nominally does not move with respect to the rotary table.

#### (2) Dynamic measurement of B-, X- and Z-axes synchronized motion

Similarly as (1), B-axis is rotated from  $B = -90^\circ$  to  $90^\circ$ , and then to  $-90^\circ$ . The three instruments were compared. Figure 6 shows the test setup with the contact R-Test instrument.

## 4. Evaluation of measured trajectories

### 4.1. Objective

In the definition in ISO 230-7 [1], radial, tangential and axial error motions of a rotary axis represent the change in the position and orientation of the axis of rotation from its axis average line. The measured sphere displacement profiles contains the influence of the position and orientation errors of the rotary axis average line (also called the position-independent geometric errors (PIGEs)). It is well recognized that the position and orientation errors of the rotary axis average line can quickly change by the thermal influence [29, 30]. For the comparison in error motions, their influence should be removed.

More importantly, the present tests can be influenced by various setup errors.

Annex D in ISO 10791-6 [9] describes the precaution on the setup errors in the ball bar tests or the R-Test, and in principle, the same applies to any sensors. For example, when the Laser R-Test, attached to the machine spindle, is applied to the test in Fig. 3, the measured displacement should be defined zero when the sphere is precisely on the spindle axis of rotation. Any alignment error changes the measured profile.

This section presents an algorithm to numerically remove the influence of the position and orientation errors of the rotary axis average line from the measured profiles. The sensors nest of the Laser R-Test (Fig. 3) is attached to the machine spindle, and thus it measures the sphere displacement in the machine coordinate system (MCS). On the other hand, the tactile R-Test sensors nest (Fig. 1) and the laser interferometer (Fig. 5) are fixed on the machine table, and thus measure the sphere displacement in the workpiece coordinate system (WCS). The WCS is a local CS that rotates with C- and B-axes. For their comparison, in accordance with ISO 10791-6 [9], the measured trajectories are converted to a) radial, b) tangential and c) axial directions of the rotary axis.

#### 4.2. Conversion to radial, tangential and axial directions of the rotary axis with eliminating the influence of position and orientation errors of rotary axis average line

As an example, consider the C-axis test by the Laser R-Test (see Fig. 3). Denote the  $k$ -th measured 3D displacement of the sphere by  ${}^r\Delta p(k) \in \mathbb{R}^3$ , when the C-axis angular position is given by  $C(k) \in \mathbb{R}$ . Note that the sphere displacement is measured in the MCS, since the Laser R-test sensors nest is installed on the machine spindle. The left-hand side superscript,  ${}^r$ , represents a vector in the MCS. Suppose that the initial sphere position at  $C(1) = 0^\circ$  in the MCS is given by  ${}^r p_0 \in \mathbb{R}^3$ . Then, the nominal sphere position in the MCS at the time  $k$  is given by:

$${}^r p^*(k) = R_c(-C(k)) \cdot {}^r p_0 \quad (1)$$

where  $R_c(-C(k)) \in \mathbb{R}^{3 \times 3}$  represents the rotation matrix around the Z-axis by the angle  $-C(k)$ . The measured displacement of the sphere in the radial and tangential direction of C-axis are respectively given by:

$$\begin{aligned} E_{\text{radial,C}}(k) &= {}^r \Delta p(k) \cdot v_{\text{radial,C}}(k) \\ E_{\text{tangential,C}}(k) &= {}^r \Delta p(k) \cdot v_{\text{tangential,C}}(k) \end{aligned} \quad (2)$$

where  $v_{\text{radial,C}}(k) = \frac{{}^r p^*(k)}{\|{}^r p^*(k)\|}$  and  $v_{\text{tangential,C}}(k) = R_c\left(-\frac{\pi}{2}\right) v_{\text{radial,C}}(k)$  are respectively a unit vector representing the radial and tangential direction of the C-axis. Note that the origin of the MCS is defined at the nominal intersection of C- and B-axes. By using  $E_{\text{radial,C}}(k)$  and  $E_{\text{tangential,C}}(k)$ , the measured sphere position is represented in radial and tangential directions with respect to the nominal position,  ${}^r p^*(k)$  by:

$$\begin{aligned} {}^r p_{\text{radial,C}}(k) &= {}^r p^*(k) + v_{\text{radial,C}}(k) \cdot E_{\text{radial,C}}(k) \\ {}^r p_{\text{tangential,C}}(k) &= {}^r p^*(k) + v_{\text{tangential,C}}(k) \cdot E_{\text{tangential,C}}(k) \end{aligned} \quad (3)$$

From the trajectory of  ${}^r p_{\text{radial,C}}(k)$ , the (X, Y) position of the C-axis average line,  ${}^r p_{\text{center,C}} \in \mathbb{R}^2$ , can be identified by solving the following problem:

$$\min_{{}^r p_{\text{center,C}}, r_C} \sum_k \left\{ \left\| \begin{bmatrix} 1 & 0 & 0 \\ 0 & 1 & 0 \end{bmatrix} \cdot {}^r p_{\text{radial,C}}(k) - {}^r p_{\text{center,C}} \right\| - r_C \right\}^2 \quad (4)$$

Then, the nominal sphere center trajectory around this identified center can be formulated by:

$${}^r \tilde{p}^*(k) = R_c(-C(k)) ({}^r p_0 - {}^r p_{\text{center,C}}) \quad (5)$$

Re-calculate the radial and tangential errors with respect to this nominal trajectory:

$$\tilde{E}_{\text{radial,C}}(k) = v_{\text{radial,C}}(k) \cdot ({}^r p_{\text{radial,C}}(k) - {}^r \tilde{p}^*(k)) \quad (6)$$

$$\tilde{E}_{\text{tangential,C}}(k) = v_{\text{tangential,C}}(k) \cdot ({}^r p_{\text{radial,C}}(k) - {}^r \tilde{p}^*(k)) \quad (7)$$

$\tilde{E}_{\text{radial,C}}(k)$  and  $\tilde{E}_{\text{tangential,C}}(k)$  respectively represent the measured tool center point profiles in radial and tangential directions of C-axis, with eliminating the influence of the position error of the C-axis average line,  ${}^r p_{\text{center,C}}$ . If error motions of linear axes (X- and Y-axes) are negligibly small, they can be seen as the radial and angular positioning error motions of C-axis. The profiles by the tactile R-Test and the laser interferometer, measured in the WCS, can be first converted to the MCS, and then the same calculation can be applied.

## 5. Experiment

### 5.1. Experimental comparison

A vertical five-axis machining center, NMV3000DCG by DMG Mori Co., Ltd., was tested. Figure 7 shows its machine configuration. The positioning resolution is 1  $\mu\text{m}$  for linear X-, Y- and Z-axes and  $0.001^\circ$  for rotary B- and C-axes.

#### (1) Dynamic measurement of C-, X- and Y-axes synchronized motion

Figure 8 compares the measured error profiles in the radial direction of C-axis,  $\tilde{E}_{\text{radial,C}}(k)$ , calculated in Eq. (6). The same test was performed by using a) the tactile R-Test instrument (in Fig. 1), b) the Laser R-Test (in Fig. 3), and c) the laser interferometer (in Fig. 5). They are shown in a polar plot format with respect to  $C(k)$ . The black full circle represents zero error, and the error in the radial direction is magnified 1,000 times (see the error scale, “10  $\mu\text{m}/\text{div}$ ”). This representation is in accordance with ISO 10791-6 [9] (Annex D). The initial sphere position at  $C(1) = 0$  was  ${}^r p_0 = [1.3, 117.8, 179.4]^T$  mm (the nominal path radius is approximately 117.8 mm) and approximately the same for all the three setups (the difference was within 2 mm, and such a small difference does not influence the test results). The command C-axis feedrate was 4,500 deg/min.

All profiles in Fig. 8 show a steady-state error in the C-axis radial direction of 30  $\mu\text{m}$  approximately. This is caused by the steady-state contouring error in the circular interpolation by X- and Y-axes due to the reduction of the gain of their closed-loop

frequency responses (the same influence can be observed in the conventional circular test with two linear axes, see [31]). Figure 9 shows the same profiles magnified near starting and reversal points. The three measuring instruments showed a good match, although they show minor differences. The following discusses possible causes for the difference:

- (1) The profile measured by the Laser R-Test (Fig. 9b) contains a higher-frequency “noise” of the amplitude up to  $10 \mu\text{m}$ . This is most likely due to the influence of the laser beam speckle.
- (2) Compared to Fig. 9c, the profile measured by the tactile R-Test (Fig. 9a) shows a small delay between CW and CCW profiles. This may be due to a synchronization error between the measured sphere displacement, and the rotary axis angular position, logged from the machine tool controller (time delay in the logging of these signals). Alternatively, it can be possibly due to the influence of the friction between the probe and the sphere. The difference between CW and CCW profiles is, however, about  $1 \mu\text{m}$ , which is not significant compared to the machine’s positioning resolution ( $1 \mu\text{m}$ ).

Figure 10 compares the measured error profiles in the axial (Z) direction of C-axis. The axial (Z) displacement,  $\tilde{E}_{\text{axial,C}}(k)$ , is plotted in a polar plot format. For the comparison in dynamic measurement, only close-up views near starting and reversal points are shown. There was a small bidirectional displacement (about  $1 \mu\text{m}$ ) before and after the reversal. Such a small displacement can be observed by all the measuring instruments. It is interesting to note that the higher frequency “noise” on the Laser R-Test measurement (Fig. 10b) seems significantly smaller than the radial profile in Fig. 9b. This is probably because the actual relative displacement of the glass sphere was smaller in the Z-direction than in X- or Y-directions (actual sphere displacement in X- or Y-directions was influenced by the position error of C-axis average line and larger, but this influence is removed in Fig. 9). Furthermore, in Fig. 10c, there is an abrupt “noise” near  $X=25 \text{ mm}$ . Its cause is not clear but a laser interferometer is typically more sensitive to a small surface disorder or contamination.

### (2) Dynamic measurement of B-, X- and Z-axes synchronized motion

The nominal path radius was approximately  $195.1 \text{ mm}$ . Figure 11 compares the measured error profiles in the tangential direction of B-axis. The tangential displacement,  $\tilde{E}_{\text{tangential,B}}(k)$ , calculated similarly as in Eq. (7), is plotted in a polar plot format with respect to  $B(k)$ . In all the three plots, the error is defined positive (outward) when the spindle is ahead of the table.

### (3) Summary

In all the tests in (1) and (2), the three measuring instruments showed similar profiles. For dynamic errors, which are evident near the starting/finishing and reversal points, the tactile R-Test show similar measuring performance as non-contact instruments. Although the manufacturers of the Laser R-Test and the laser interferometer

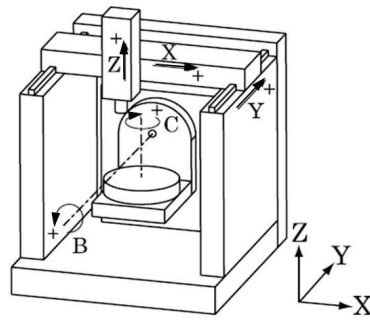


**Figure 7.** Five-axis machine configuration considered in this paper.

do not disclose the bandwidth of these sensors, it is typically much larger than the bandwidth of a tactile displacement sensor. The experiment in Section 5.2 will show that the bandwidth of the tactile displacement sensor (Heidenhain ST1288) is about 54 Hz. Despite of this limited bandwidth, similar dynamic responses in Figs. 9 to 11 show that the bandwidth of the tactile R-Test was sufficiently high for a large portion of the frequency components contained in these particular tests. If the machine's motion contains frequency components higher than the spring's bandwidth, the tactile R-Test may be subject to larger measurement error. This will be further studied in the following subsection.

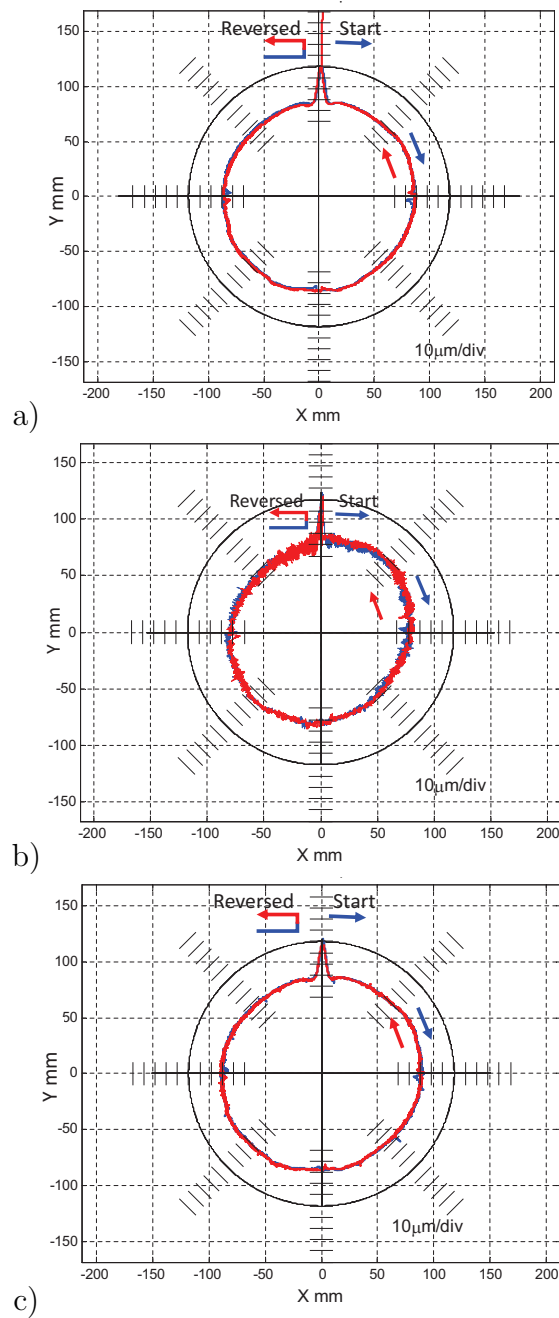


**Figure 8.** Error profiles in the radial direction of C-axis measured by a) the tactile R-Test, b) the Laser R-Test, and c) the laser interferometer.

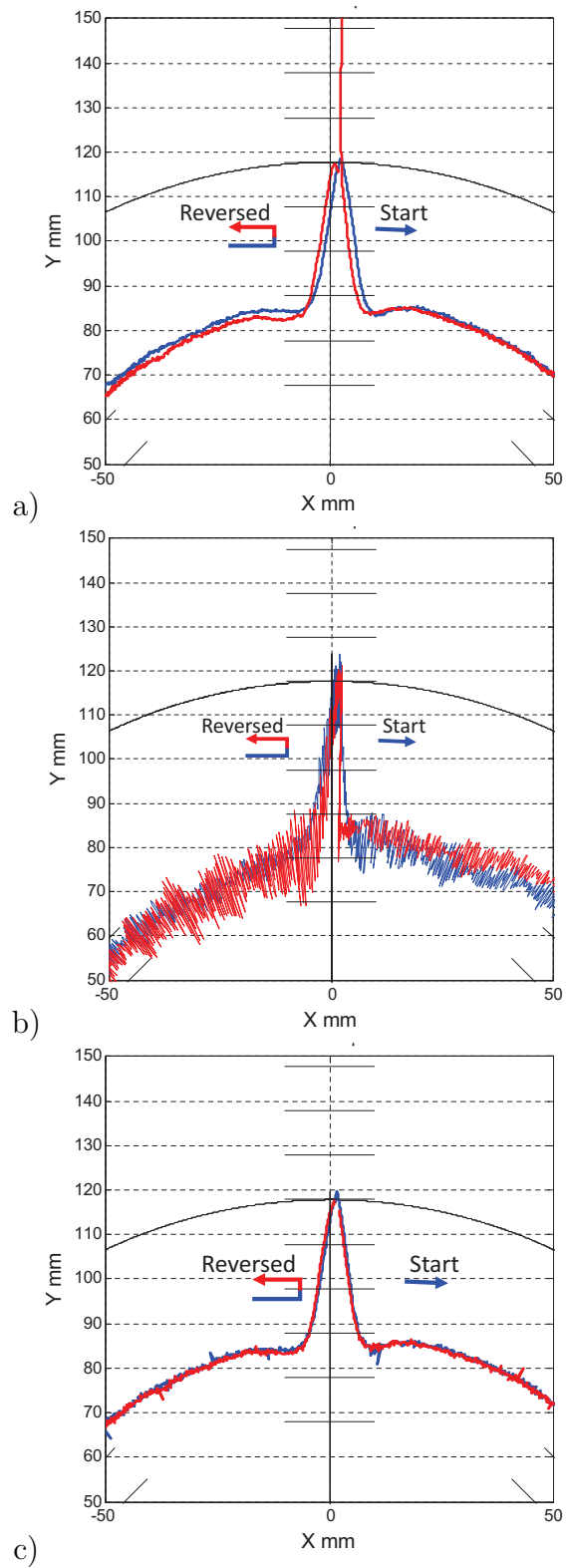


**Figure 9.** Close-up view of Fig. 8 near starting/finishing and reversal points. Error profiles in the C-axis radial direction measured by a) the tactile R-Test, b) the Laser R-Test, and c) the laser interferometer.

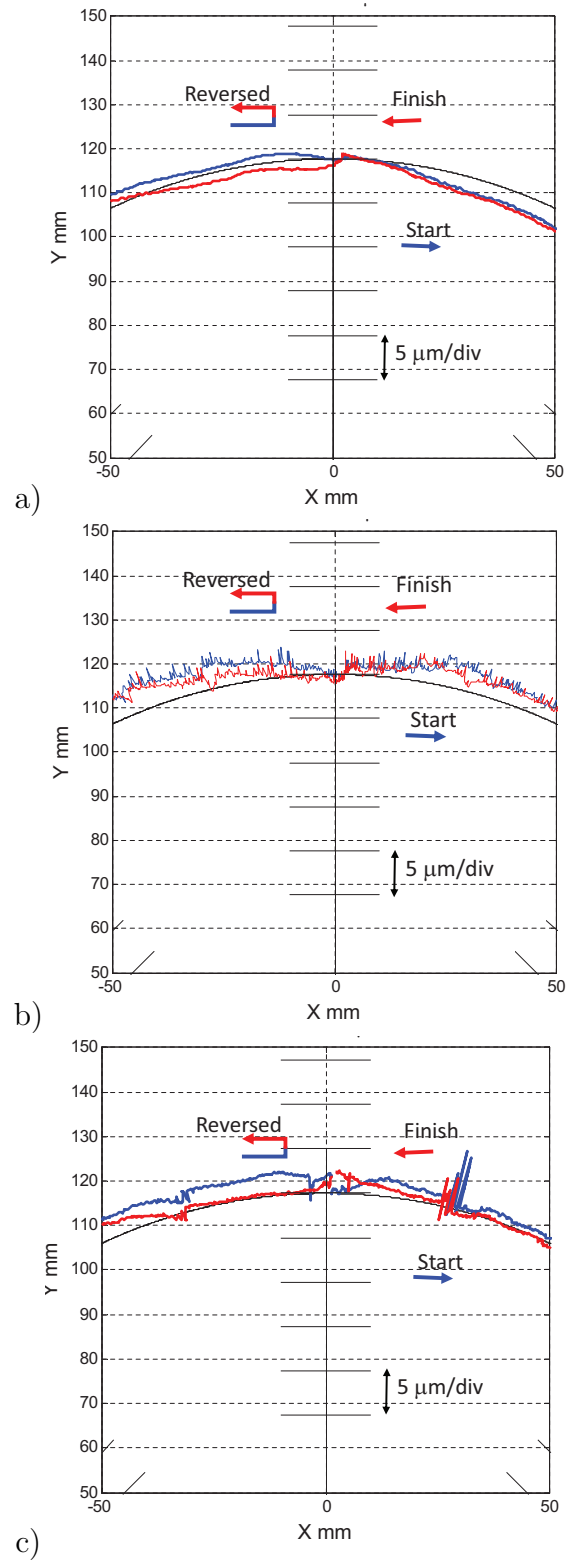


**Figure 10.** Error profiles in the C-axis axial (Z) direction, closed-up near starting and reversal points, measured by a) the tactile R-Test, b) the Laser R-Test, and c) the laser interferometer.



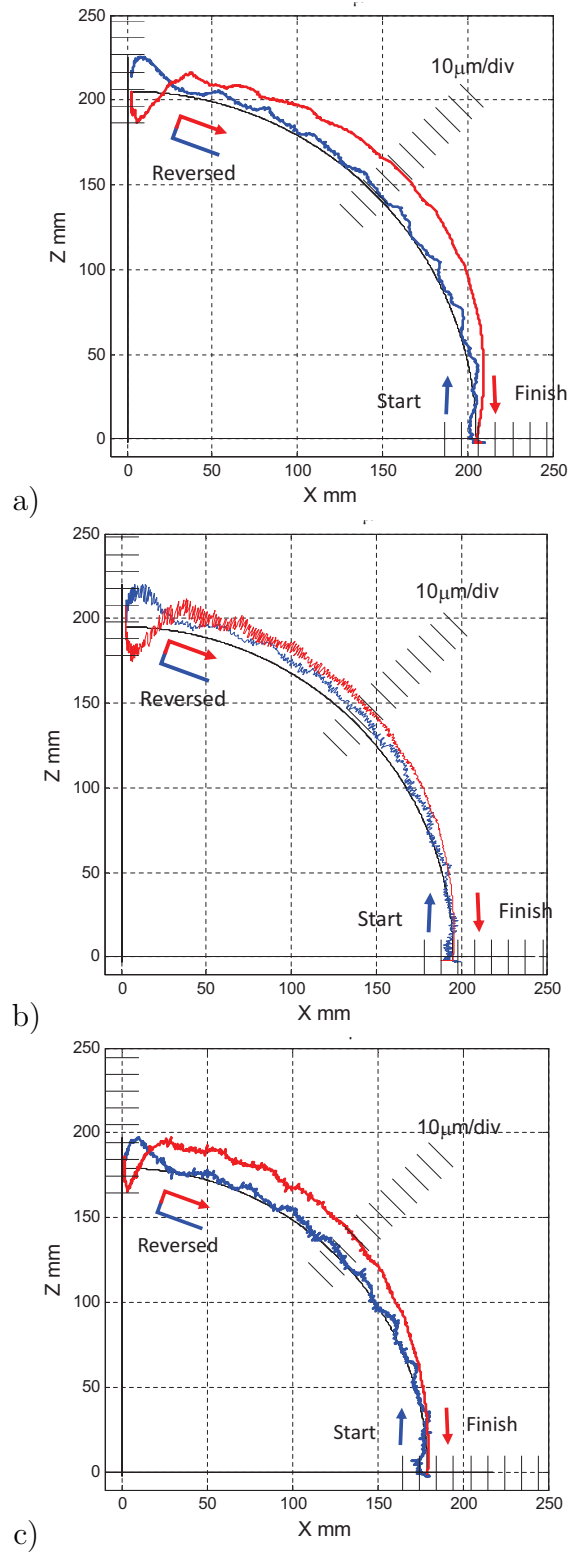


**Figure 11.** Error profiles in the tangential direction of B-axis measured by a) the tactile R-Test, b) the Laser R-Test, and c) the laser interferometer.

## 5.2. Measurement of frequency response of the tactile R-Test

### (1) Measurement setup

As shown in Fig. 2, the tactile linear displacement sensor pushes the plunger to the target surface by a leaf spring. Its stiffness limits the measurement bandwidth. Non-contact optical displacement sensors do not have such a spring and thus can have significantly larger bandwidth, which is potentially advantageous in dynamic measurement. This subsection presents an experiment to measure the bandwidth of the tactile linear displacement sensor.

Figures 12 and 13 show the experimental setup. The linear displacement sensor, ST1288, used in the tactile R-Test instrument, was tested. A cylinder of the nominal diameter 10 mm was installed on the machine tool spindle. A flat-ended measuring contact of the linear displacement sensor touches the cylinder. First, its radial runout is measured by rotating the spindle in a sufficiently low speed. It was 58  $\mu\text{m}$ .

The spindle speed was increased from 0 Hz with an increment of 3 Hz ( $180 \text{ min}^{-1}$ ). At every rotation speed, the displacement was continuously measured for several rotations. It was verified by an experiment that the change in the spindle's actual radial error motion is sufficiently small for the frequencies up to 60 Hz. Thus, the amplitude of the measured displacement gives the gain of the frequency response of the linear displacement sensor at the given frequency. By increasing the frequency, the gain profile can be obtained.

### (2) Result

From the spindle speed 3 Hz to 51 Hz ( $=3,060 \text{ min}^{-1}$ ), the amplitude of the measured displacement profiles was approximately the same as the quasi-static runout, 58  $\mu\text{m}$ . As an example, Fig. 14a shows the measured displacement profile at 45 Hz. At the spindle speed 54 Hz ( $=3,240 \text{ min}^{-1}$ ), as shown in Fig. 14b, the measured displacement became significantly larger than the actual runout. This is because the probe lost the contact with the target surface, due to the finite stiffness of the plunger spring. At the frequencies equal to or higher than 54 Hz, the amplitude was similarly much larger than 58  $\mu\text{m}$ , and thus the test was terminated.

This test result shows that this linear displacement sensor's bandwidth was 51 Hz. In dynamic tests presented in Section 4, when the motion of linear and rotary axes contains the components of the frequencies higher than 51 Hz, this tactile displacement sensor can be subject to significant measurement errors, and non-contact sensors should be used. However, in the particular test conditions in Section 4, such influence was not evident and the tactile R-Test showed sufficient dynamic measurement performance.

## 6. Conclusion

This paper experimentally compared the measuring performance of the R-Test instruments with 1) tactile linear displacement sensors, 2) laser displacement sensors

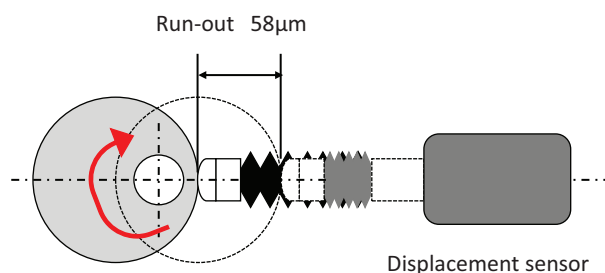


**Figure 12.** Setup to measure the bandwidth of a tactile linear displacement sensor.

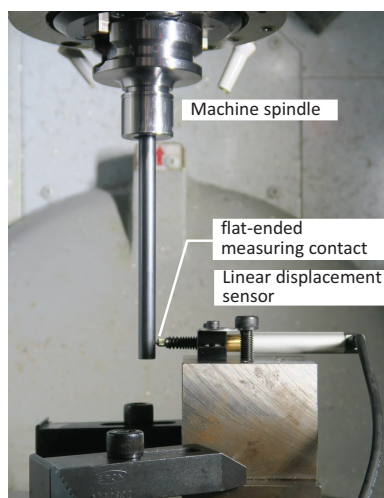


**Figure 13.** Experimental setup.

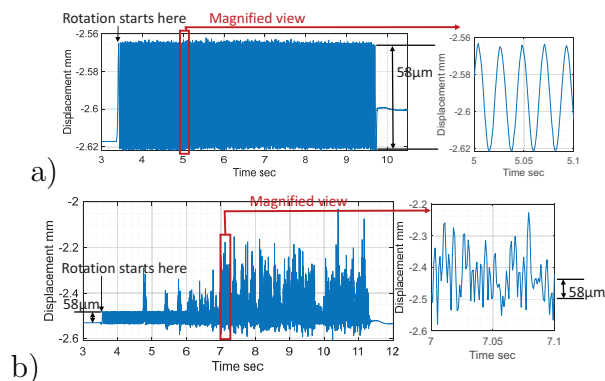


**Figure 14.** Measured displacement profiles at the spindle rotation speed a) 45 Hz and b) 54 Hz. At sufficiently small spindle speed, the radial runout was 58  $\mu\text{m}$ .

based on the refraction in a glass ball lens (Laser R-Test), and 3) laser interferometers, in dynamic measurement of synchronization error of a rotary and linear axes. Its contributions and findings are summarized as follows:

(1) For clearer comparison, an algorithm to eliminate the influence of setup errors, as

well as the position error of the rotary axis average line, is presented.

- (2) It was experimentally verified that the trajectories, measured by the three R-Test instruments, show a good match. The profiles measured by the Laser R-Test contains a higher-frequency “noise” of the amplitude up to 10  $\mu\text{m}$ , which is attributable to the laser beam speckle influence. The limited bandwidth of a tactile linear displacement sensor (see below) can potentially cause a measurement error particularly for dynamic profiles. In the test conditions presented in this paper, however, such influence was not evident, and the tactile R-Test showed a good dynamic measurement performance.
- (3) A tactile displacement sensor pushes its measuring contact to the target surface by a spring. The stiffness of the spring determines the bandwidth of the sensor. When the target’s motion has the frequency higher than the spring’s bandwidth, the probe can lose the contact with the target surface, which causes large measurement error. This paper presented a simple experiment to measure this bandwidth. A non-contact displacement sensor does not have such a limitation.

## Declarations

**Funding:** The authors declare that no funds, grants, or other support were received during the preparation of this manuscript

**Competing interests:** The authors declare no competing interests.

**Availability of data and material:** The data and material that support the findings of this study are available on request.

**Code availability:** Not applicable.

**Ethics approval:** Not applicable.

**Consent to participate:** Written informed consent for publication was obtained from all participants.

**Consent for publication:** Written informed consent for publication was obtained from all participants.

**Authors’ contributions:** All authors contributed to the study conception and design. Experiments, data collection and analysis were performed by Soichi Ibaraki and Koki Onodera. Wen-Yuh Jywe, Chia-Ming Hsu, and Yu-Wei Chang designed and constructed the Laser R-Test and analyzed experimental data. The first draft of the manuscript was written by Soichi Ibaraki and all authors commented on previous versions of the manuscript. All authors read and approved the final manuscript.

## References

- [1] ISO 230-7:2015, Test code for machine tools – Part 7: Geometric accuracy of axes of rotation.
- [2] ISO 10791-1:2015, Test conditions for machining centres – Part 1: Geometric tests for machines with horizontal spindle (horizontal Z-axis).
- [3] Weikert S (2004) R-Test, a New Device for Accuracy Measurements on Five Axis Machine Tools, *Annals of CIRP – Manufacturing Technology*, 53(1): 429–432.
- [4] Bringmann B, Knapp W (2006) Model-based ‘Chase-the-Ball’ calibration of a 5-axis machining center, *Annals of CIRP – Manufacturing Technology*, 55(1): 531–534.
- [5] Ibaraki S, Oyama C, Otsubo H (2011) Construction of an error map of rotary axes on a five-axis machining center by static R-test, *International Journal of Machine Tools and Manufacture*, 51(3): 190-200.
- [6] Hong C, Ibaraki S (2012) Graphical presentation of error motions of rotary axes on a five-axis machine tool by static R-test with separating the influence of squareness errors of linear axes, *International Journal of Machine Tools and Manufacture*, 59: 24-33.
- [7] Ibaraki S, Nagai Y, Otsubo H, Sakai Y, Morimoto S, Miyazaki Y (2015) R-Test Analysis Software for Error Calibration of Five-Axis Machine Tools –Application to a Five-Axis Machine Tool with Two Rotary Axes on the Tool Side–, *International Journal of Automation Technology*, 9(4): 387-395

- [8] Florussen G, Houben K, Spaan H, Spaan-Burke T (2020) Automating Accuracy Evaluation of 5-Axis Machine Tools, *International Journal of Automation Technology*, 14(3): 409-416.
- [9] ISO 10791-6:2014, Test conditions for machining centres – Part 6: Accuracy of speeds and interpolations.
- [10] Lei WT, Hsu YY (2002) Accuracy test of five-axis CNC machine tool with 3D probe-ball. Part I: design and modeling, *International Journal of Machine Tools and Manufacture*, 42(10): 1153-1162.
- [11] Ihara Y, Hiramatsu Y (2011) Design of Motion Accuracy Measurement Device for NC Machine Tools with Three Displacement Sensors, *International Journal of Automation Technology*, 5(6): 847-854.
- [12] Zargarbashi SHH, Mayer JRR (2009) Single setup estimation of a five axis machine tool eight link errors by programmed end point constraint and on the fly measurement with Capball sensors, *International Journal of Machine Tools and Manufacture*, 49: 759-766.
- [13] Hong C, Ibaraki S (2013) Non-contact R-test with laser displacement sensors for error calibration of five-axis machine tools, *Precision Engineering* 37 (1): 159-171.
- [14] Guo Y, Song B, Tang X, Zhou X, Jiang Z (2021) A calibration method of non-contact R-test for error measurement of industrial robots, *Measurement*, 173 (2021), 108365
- [15] Jiang L, Peng B, Ding G, Qin S, Zhang J, Yong L (2020) Optimization method for systematically improving non-contact R test accuracy, *International Journal of Advanced Manufacturing Technology*, 107:1697-1711.
- [16] Ibaraki S, Kitagawa T, Kimura Y, Nishikawa S (2017) On the limitation of dual-view triangulation in reducing the measurement error induced by the speckle noise in scanning operations, *International Journal of Advanced Manufacturing Technology*, 88(1): 731-737.
- [17] Nishiguchi N, Ryuta S, Shirase K (2016) Evaluation and compensation of dynamic behavior of rotary axis by motion direction changes in 5-axis controlled machining center, *Journal of the Japan Society of Precision Engineering*, 82(10) 913-918 (in Japanese)
- [18] Nishiguchi N, Ryuta S, Shirase K (2017) Evaluation of axial displacement caused by rotary axis motion direction change in five-axis controlled machining centers, *Journal of the Japan Society of Precision Engineering*, 83(9) 893-898 (in Japanese)
- [19] Jiang Z., Ding J., Zhang J., Ding Q., Li Q., Du L., Wang W. (2019) Research on detection of the linkage performance for five-axis CNC machine tools based on RTCP trajectories combination, *International Journal of Advanced Manufacturing Technology*, 100, 941-962
- [20] ISO 10791-7:2020, Test conditions for machining centres – Part 7: Accuracy of finished test pieces
- [21] Wang W., Jiang Z., Jiang Z., Tao W. (2015) A new test part to identify performance of five-axis machine tool – Part II validation of S part, *International Journal of Advanced Manufacturing Technology*, 79 (5-8) 739-756
- [22] Chanal H., Duc E., Chevalier A. (2022) Studying the influence of the machining process on the geometrical defects of the standardized S-shape test part, *Precision Engineering*, 75, 193-209
- [23] Li Q., Ibaraki S., Wang W. (2022) Proposal of a Machining Test to Evaluate Dynamic Synchronization Error of Rotary and Linear Axes With Reversal of Rotation Direction, *Transactions of the ASME Journal of Manufacturing Science and Engineering*, 144(4) 041002.
- [24] Jywe WY, Hsu TH, Liu CH (2012) Non-Bar, an Optical Calibration System for Five-axis CNC Machine Tools, *International Journal of Machine Tools and Manufacture*, 59, 16-23.
- [25] Lin MT, Wu SK (2013) Modeling and analysis of servo dynamics errors on measuring paths of five-axis machine tools, *International Journal of Machine Tools and Manufacture*, 66: 1-14.
- [26] Tran CS, Hsieh TH, Jywe WY (2021) Laser R-Test for Angular Positioning Calibration and Compensation of the Five-Axis Machine Tools, *Applied Science*, 11(20), 9507
- [27] Dr. Johannes Heidenhain, Linear gauges (catalog, April 2017), [https://www.heidenhain.com/en\\_US/products/length-gauges/](https://www.heidenhain.com/en_US/products/length-gauges/) (accessed on March 2023).
- [28] Keyence, SI-F Series Catalog, <https://www.keyence.com/products/measure/spectral/si-f/models/si-f10/> (accessed on March 2023).

- [29] Onishi S., Ibaraki S., Kato T., Yamaguchi M., Sugimoto T. (2022) A self-calibration scheme to monitor long-term changes in linear and rotary axis geometric errors, *Measurement*, 196, 111183.
- [30] Ibaraki S, Inui H, Hong C, Nishikawa S, Shimoike M. (2019) On-machine identification of rotary axis location errors under thermal influence by spindle rotation, *Precision Engineering*, 55, 42-47.
- [31] ISO 230-4: 2022, Test code for machine tools – Part 4: Circular tests for numerically controlled machine tools